

Regional loss of the mitochondrial membrane potential in the hepatocyte is rapidly followed by externalization of phosphatidyl serines at that specific site during apoptosis.

W. Marty Blom, Hans J.G.M. de Bont and J.Fred Nagelkerke

Division of Toxicology, Leiden-Amsterdam Center for Drug Research, Leiden University, Leiden, The Netherlands.

Address for correspondence: J.Fred Nagelkerke, Division Toxicology, LACDR, Gorlaeus Laboratories, P.O. Box 9502, 2300 RA, Leiden, The Netherlands.

Tel: 31-71-5276226; FAX: 31-71-5274277; E-mail: nagelker@lacdr.Leidenuniv.nl

Running title: defective mitochondria and phosphatidyl serine exposure

Abstract

The spatio-temporal relationship between a decrease in the mitochondrial membrane potential (MMP) and externalization of phosphatidyl serines (PS) during induction of apoptosis was investigated in single freshly isolated hepatocytes. Apoptosis was induced in the hepatocytes in three different ways: attack by activated Natural Killer cells, exposure to ATP or exposure to the inhibitor of protein synthesis cycloheximide. Fluorescence microscopy showed staining of externalized PS at those areas where the staining for MMP was lost while in other areas the mitochondria remained intact for longer periods of time, indicating coupling between local loss of MMP and local PS exposure. To discriminate whether the decrease in MMP itself or a decrease in ATP induced PS externalization, hepatocytes were treated with rotenone, which resulted in a rapid collapse of cellular ATP but left the MMP intact for a much longer period. Addition of fructose prevented the decrease of ATP to approximately 30% and also delayed the collapse of the MMP. This indicates that ATP was needed for the maintenance of the MMP probably via reverse action of the ATP synthase. In a subsequent study hepatocytes were incubated with NK cells for induction of apoptosis followed by addition of rotenone to deplete ATP. Under these conditions the PS staining co-localized with mitochondrial MMP indicating that PS externalization does not require a collapse in MMP. Moreover, exposure of PS was evenly distributed over the whole plasma membrane.

In conclusion, we propose that after an apoptotic stimulus some mitochondria start to loose their MMP which results in cessation of ATP production and perhaps even consumption of ATP. This results in an overall decrease in cellular ATP. ATP-consuming enzyme reactions most distal from still intact mitochondria will be most sensitive to such

a decrease. Apparently the translocase that keeps phosphatidyl serines inward oriented is such a sensitive enzyme.

Abbreviations

A-NK interleukin-2-activated natural killer cells; ANV annexin V; BSA bovine serum albumin; CLSM confocal laser scan microscopy; IL interleukin; MHC major histocompatibility complex; MMP mitochondrial membrane potential; PI propidium iodide; PS phosphatidyl serine; TMR tetramethylrosamine; TOTO-3 1,1'-(4,4,8,8-tetramethyl-4,8-diazaundecamethylene)bis[4-(3-methyl-2,3-dihydrobenzo-1,3-thiazolyl-2-methylidene)quinolinium] tetraiodide; VIFM video-intensified fluorescence microscopy.

Keywords

Mitochondrial membrane potential; phosphatidyl serines; apoptosis; hepatocytes

Introduction

It has been demonstrated in many cell types, using a large variety of inducers that mitochondria often play a crucial role in development of apoptosis and necrosis (reviewed in 1,2). Already in the 1980s a relation was observed between elevated calcium concentrations and the Mitochondrial Membrane Potential (MMP) on the one hand and cell death on the other hand upon exposure of hepatocytes to toxic compounds or after ischemia-reperfusion (3). It was shown that opening of a high conductance permeability transition (PT) pore after oxidative stress in the mitochondrial inner membrane abruptly increases the permeability of the mitochondrial inner membrane to solutes of molecular mass up to 1500 Da (4,5). The opening of the pore is associated with a collapse of the MMP, perturbation of intracellular and mitochondrial Ca^{2+} homeostasis and subsequently cell death. The mitochondrial outer membrane is also the site of competition between the pro- and anti-apoptotic proteins of the Bcl-2 family and is associated with the opening of the pore (6-9). Moreover, the mitochondria are a source of a number of the Bcl-2 family members and, in lymphoid cells, of the Apoptosis Inducing Factor (AIF), a protein associated with opening of the pore and induction of apoptosis (10). Other mitochondrial factors that are associated with liver apoptosis in vivo are proteases that are released during cholestasis (11). Finally several studies showed that after induction of apoptosis mitochondria release cytochrome c (12) which is associated with opening of the mitochondrial pore (13). Cytochrome c forms a complex with APAF-1, procaspase-9 and ATP. Formation of this complex, the apoptosome, leads to formation of active caspase-9 that can subsequently activate other caspase proteins. In this way the apoptotic signal is amplified (reviewed in (14)). Associated with the activation of the caspases is exposure

of phosphatidyl serines (PS) in the outer leaflet of cells (15,16). These molecules function as a signal for macrophages or other cells from the reticuloendothelial system to engulf and digest apoptotic bodies (17). In this way release of intracellular components and a subsequent immunological reaction is prevented. The exposure of PS is either the result of inhibition of an ATP-dependent aminophospholipid transporter (18, 19) or activation of a calcium-dependent scramblase (20-22). In addition, synthesis of PS through a calcium-dependent exchange of the polar head group of pre-existing phospholipids has been described (23).

In thymocytes exposure of PS occurs only in those cells that have lost their MMP (15,24). In other cell types the opposite was found: in L929sAh cells transfected with the FAS-receptor and treated with anti-FAS initially PS were exposed followed later by a drop in MMP (25). We described the involvement of the mitochondria in the induction of apoptosis in hepatocytes after attack by interleukin-activated Natural Killer (A-NK) cells (16). FACS-analysis after staining for extracellular oriented PS with fluorescent-labeled Annexin V (ANV) demonstrated that A-NK cells induced apoptosis in the hepatocytes (10% apoptotic cells after 30 minutes and 38% after 60 minutes of co-incubation) In these apoptotic cells the overall MMP was approximately 60% of the value as compared to non-apoptotic hepatocytes. The decrease in MMP and exposure of PS in hepatocytes is apparently tightly coupled because all cells with a lowered MMP exposed PS. In comparison with other studies (15,24,25) the decrease in MMP was relatively moderate and the exposure of PS was very rapid. Microscopical examination showed that ANV staining was unevenly distributed over the cell membrane.

To gain more insight in the spatial-temporal relationship between a decrease in the MMP on the one hand and exposure of PS on the other hand the present study was undertaken. Time-lapse video microscopy and confocal laser scan microscopy of hepatocytes that were attacked by A-NK cells was performed. In addition, two totally unrelated apoptosis-inducing stimuli were applied: addition of extracellular ATP or cycloheximide (26,27). We report that in all cases a local loss of MMP of a limited number of mitochondria in the cell results, within minutes, in exposure of phosphatidyl serines at that particular spot.

Materials and methods

Materials

Collagenase, recombinant protein ANV and 4-(2-hydroxyethyl)-1-piperazine-N-(2-ethanesulfonic acid) (HEPES) were obtained from Boehringer (Mannheim, Germany). Tetramethyl rosamin (TMR), rhodamin 123, propidium iodide (PI), TOTO-3 and the AlexaTM protein labeling kit were from Molecular Probes (Leiden, The Netherlands). Fluorescent ANV was prepared by labeling with AlexaTM488 or AlexaTM633. Bovine serum albumin (type V), the luciferin/luciferase kit and poly-L-lysine were from SIGMA (St. Louis, MO, USA). Mouse anti-rat mAb OX18 (anti-total rat MHC class I) was prepared as described before (28).

Methods

Isolation and activation of natural killer cells

Isolation of natural killer cells and activation of these cells were done as described in (16). Briefly, a cell suspension was prepared from spleen isolated from a 4-5 months old male Wag rat (RT1^u), a Wistar-derived strain, purchased from Charles Rivers Wiga (Schulzfeld, Germany). The splenocytes were separated from other cells (i.e. B cells, macrophages) by nylonwool adherence. The non-adherent cells contained approximately 30% A-NK cells, which were collected and cultured in RPMI-1640, Dutch modification (Invitrogen, Breda, The Netherlands), supplemented with 10% (v/v) heat-inactivated fetal calf serum (FCS), 2 mM glutamine, 50 µg/ml streptomycin and 50 U/ml penicillin (all Invitrogen). The culture medium was supplemented with 1000 Cetus Units/ml human recombinant Interleukin-2 (rIL-2) (Chiron, Amsterdam, The Netherlands), and 50 µM 2-

mercaptoethanol. After 24 hrs non-adhering cells were removed and the remaining adhering cells, A-NK cells, were cultured for another 6 days. The population thus obtained consisted for $\geq 95\%$ of CD161A positive cells and for $\leq 5\%$ of T cell receptor-positive cells.

Isolation and incubation of rat hepatocytes

Liver parenchymal cells were isolated by collagenase perfusion from male Wistar rats (200-230 gr.) (29), purchased from Charles Rivers Wiga (Schulzfeld, Germany) and housed at least one week at the animal facilities of the Sylvius Laboratories. The rats were fed *ad libitum* and kept at a 12-hour day-night cycle. Prior to the experiment the rats were fasted for 24 hours. Viability of the freshly isolated cells was $>95\%$ as determined by Trypan Blue exclusion. After isolation cells were kept on ice until use.

Incubation of hepatocytes and A-NK cells

To allow non-self recognition and induce the cytotoxic response by A-NK cells, the MHC class I protein of hepatocytes was blocked with the OX18 antibody (27). This masking leads to recognition of the target cell as foreign and activation of the killing machinery (29). The liver cells were preincubated with the OX18 antibody at 4°C for 45 minutes in Hanks'/HEPES buffer (pH 7.4, 4°C) composed of 120 mM NaCl, 5 mM KCl, 4.2 mM NaHCO_3 , 1.2 mM NaH_2PO_4 , 1.3 mM CaCl_2 , 0.4 mM MgSO_4 , 25 mM HEPES supplemented with 10 mM glucose and 1% (w/v) bovine serum albumin, gassed for 30 min with 95% O_2 /5% CO_2 . Then, cells were washed and resuspended in either William's E

supplemented with 10% FCS or the Hanks'/HEPES buffer supplemented with 1% (w/v) bovine serum albumin.

For microscopical experiments isolated liver cells were allowed to attach to circular glass cover slips coated with poly-D-lysine (1 mg/ml in water) (16). The cover slips were placed in a microscope chamber and 500 μ l cell suspension (3.0×10^5 cells/ml) was carefully added to the glass cover slip; the hepatocytes were allowed to attach for 45 min. The cells were kept at 37°C throughout the experiment. The experiments with the A-NK cells were started by removal of the medium and addition of A-NK cells in William's E supplemented with 10% FCS in the effector:target ratio of 20:1. This ratio was chosen because previous experiments showed that it resulted in apoptosis in a large number of hepatocytes (16). In other experiments ATP or cycloheximide were directly added to the cells.

Batch incubations were performed in the same Hanks' buffer on a rotary shaker that was kept at 37°C. Cells were incubated at a density of 3.0×10^5 cells/ml. At the selected intervals 0.5 ml samples were taken for flow cytometry and ATP determinations.

Imaging techniques

The video microscopy system consisted of an IM35 inverted microscope with a 100 Watt mercury arc lamp (Zeiss, Oberkochen, FRG) and a Nikon 40x\1.4 NA CF Fluor objective. ANV staining was detected using a 475 nm band pass filter for excitation, a 510 nm dichroic mirror and a 540 nm band pass emission filter. Tetramethyl-rosamine (TMR) was visualized using a 535 nm band pass filter for excitation, a 580 nm dichroic mirror and a 590 nm long pass filter for emission. Images were recorded using a CCD instrumentation camera, controlled by a CC200 camera controller (Photometrics, Tucson, AZ).

For confocal laser fluorescence microscope (CLSM) an upgraded Bio-Rad MRC-600 system was used (31). The first filter block of the CLSM contained a triple dichroic mirror (488/543/633) and an emission filter (488/543/633). ANV was excited with the 488 argon laser, TMR with the 543 nm HeNe laser and TOTO-3 with the 633 nm HeNe laser.

Staining techniques

PS externalization and plasma membrane permeabilization

Exposition of PS on the extracellular side of the plasma membrane of hepatocytes was visualized by staining PS with ANV labeled with fluorescent AlexaTM488 (1 µg/ml ANV and AlexaTM488 in a stoichiometric complex of 1:1) (4). 0.2 µl ANV and 2 µl of a 5 mM solution of the cell-impermeable dye TOTO-3 were added to 500 µl of cell suspension in the incubation chamber of the microscope.

Determination of the relation between externalization of the phosphatidyl serines, mitochondrial membrane potential and cell death.

Hepatocytes were pre-incubated for 15 minutes with 0.2 µM TMR. Subsequently ANV and TOTO-3 were added. After recording of the baseline level of TMR the apoptotic stimuli were given.

Determination of the degree of co-localization of fluorescent signals of different dyes

Co-localization of the signals was measured by comparing the equivalent pixel positions in each image and generation of a co-localization scatter plot using Image Pro software (Media Cybernetics, Silver Spring, USA). These scatter plots were analyzed using

Pearson's correlation. The result of this analysis is a number between +1 and -1. The former indicates perfect correlation and the latter absolute no correlation (32,33).

Determination of the relation between externalization of the phosphatidyl serines, intracellular free calcium $[Ca^{2+}]_i$ and cell permeabilization.

For determination of intracellular free calcium the hepatocytes were loaded with 40 μ M Fura-2AM for 30 minutes. Then, the cells were washed carefully with Hanks'/HEPES buffer at 37 °C. Next, ANV and A-NK cells were added. From a group of cells the 470 nm emission images after 340 and 380 nm excitation were recorded using a dichroic mirror of 395 nm and a 470 nm long pass emission filter. Images were corrected by background subtraction before calculation of the ratio images. Ratio images of the 340/380 nm excitation were determined by division of the 340 nm image by the 380 nm image on a pixel-to-pixel basis. The intracellular free calcium concentration was calculated using the equation $[Ca^{2+}]_i = K_d * \beta * [(R - R_{min}) / (R_{max} - R)]$, with $K_d = 224$ nM as the equilibrium dissociation constant for Ca^{2+} and Fura-2. R_{min} is the ratio F_{340}/F_{380} at zero calcium; R_{max} is the ratio F_{340}/F_{380} at saturating calcium; β is the ratio F_{380} (zero calcium)/ F_{380} (saturating calcium); and F is the pixel fluorescence intensity.

Flow cytometric analysis of the percentage viable, apoptotic and dead hepatocytes

The MMP of viable, apoptotic and dead cells was determined by flow cytometric analysis using ANV, Propidium Iodide (PI) and rhodamine 123 as described earlier (16). Briefly, after addition of ANV, rhodamine 123 and PI the hepatocytes were incubated for 15 minutes on ice in the dark. The fluorescence of individual cells was analyzed using a

FACScalibur flow cytometer (Becton Dickenson, San Jose, CA, USA), using the CellQuest program.

Determination of ATP in the hepatocytes

Samples of the hepatocytes were snap-frozen in liquid N₂. Determination of ATP was started by addition of HClO₄ to the frozen cells. Subsequently KPO₄ was added, after 10 minutes pH was neutralized with KOH. The tubes were centrifuged; ATP was determined in the supernatant using the Sigma luciferin/luciferase kit

Statistics

Values are expressed as mean \pm s.d.. The statistical evaluation was performed with an unpaired two-tailed Student t-test.

Results

Freshly isolated rat hepatocytes were loaded with TMR to visualize effects on the MMP; in addition, ANV labeled with Alexa 488 was added to stain external PS. The hepatocytes were attached to a cover slip mounted at the bottom of the incubation chamber; after recording of baseline values the A-NK cells were added as a suspension to the chamber and, therefore, it took some time before a contact between the hepatocytes and A-NK cells had been established. Figure 1 shows that 17 minutes after the addition of the A-NK cells such a contact was made. At this time point the morphology of the hepatocyte was still normal (fig 1, bottom row). However, 15 minutes later (32') the hepatocyte had become apoptotic showing numerous blebs. At this time-point at certain sites the MMP was dissipated (fig1, third row). This was followed 6 minutes (38') later by the first staining of PS (fig1, second row; hardly visible). These processes, decrease in MMP and externalization of PS, continued progressively. Because also TOTO-3 was added the absence of a nuclear staining in the images indicates that up till 94 minutes no secondary necrosis had occurred: the cells were still intact. The merged images of the green MMP signal and the red PS signal are shown in the top row. If these signals co-localize the merged signal becomes yellow. The absence of such staining indicates that only at the area where mitochondria had lost their MMP externalization of PS occurred.

To acquire more detailed images we used the confocal laser scan microscope (CLSM). Hepatocytes were incubated under the same conditions as described above. Figure 2a shows the MMP and 2b the externalized PS. As can be seen in the merged figure 2c the signals do not co-localize confirming the finding that PS only externalize in the vicinity

of defective mitochondria. The co-localization was further analyzed using Pearson's correlation that is discussed at the end of this section.

To test the specificity of the response, apoptosis was induced in hepatocytes with cycloheximide, a protein synthesis inhibitor. Figure 3 shows a CLSM image taken 55 minutes after the addition of cycloheximide. The arrows in 3d point at the apoptotic cells. These cells have a lowered MMP and are high in ANV-staining; the merged image again indicates no co-localization of the two signals. Identical results were found when apoptosis was induced using addition of extracellular ATP (fig 4). These results show that three completely different apoptotic signals had the same effect: externalization of PS in the near vicinity of defective mitochondria. A possible explanation for this phenomenon could be a local decrease in ATP around defective mitochondria. The enzyme that maintains the asymmetric orientation of PS, aminophospholipid translocase needs ATP for its activity. The most direct approach to investigate the role of ATP would have been intracellular determination of the concentration using a cell permeable probe like those used for determination of Ca^{2+} or MMP. Unfortunately such a probe does not exist yet. Therefore, we chose another approach: depletion of ATP without collapse of the MMP by using the mitochondrial inhibitor rotenone. First, in batch incubations of hepatocytes, the effect of rotenone on intracellular ATP and MMP was determined. Cells were incubated and at different time points two samples were taken. One was immediately snap-frozen for ATP determination. The second was incubated with ANV, rhodamine 123 and PI for flow-cytometrical analysis as described in Materials and Methods. Figure 5 shows that even at 10 μM rotenone ATP levels were less than 15% of control within 30 minutes. In contrast the MMP remained largely intact for more than 2

hours (fig 5). Interestingly, addition of fructose prevented the decrease in ATP to about 50% and moreover, delayed the decrease in the MMP. A significant increase in the number of dead cells as a result of rotenone exposure occurred in parallel with the (late) decrease in MMP. At all time points neither in the control nor in the cells incubated with rotenone more than 1% of the cells were apoptotic, indicating that a decrease in cellular ATP is not sufficient to induce apoptosis. Subsequently hepatocytes, were co-incubated with A-NK cells to induce apoptosis and after 15 minutes rotenone was added to deplete ATP and the localization of PS-staining and MMP staining was determined in apoptotic cells. Figure 6a shows the MMP and 6B the localization of the PS. In figure 6c these images were merged; it is evident that both stainings overlap. To further substantiate this the Pearson correlations of this image and of the image depicted in fig 1c were calculated. The average value of 1c was 0.15 ± 0.05 while the value for 6c was 0.75 ± 0.07 . This indicates that indeed there was much more overlap in staining after treatment with rotenone. Furthermore, comparison of figures 1b and 6b shows that PS staining was patchy in the former while in rotenone-treated cells the whole plasma membrane was uniformly stained. When hepatocytes were incubated with rotenone and fructose and A-NK cells similar images were obtained in which MMP and PS-staining were co-localized. The prevention of the decrease in ATP was not sufficient to prevent the PS-externalization. In the presence of rotenone and fructose or rotenone alone the same percentage of the cells became apoptotic and necrotic. A 3-D image of figure 6b is available on our web site <http://wwwpharm.leidenuniv.nl/lacdrhomepage/divisions/toxicology/nk2.htm>.

To investigate the role of intracellular free calcium hepatocytes were loaded with fura-2-AM and incubated with the A-NK cells in the presence of ANV. Initially the same magnification was used as in figures 2-4. Using video microscopy, in many cells an increase in the intracellular calcium concentration was observed but no shifts in the fura-2-signal at specific locations inside the cell occurred: the calcium changes were homogeneous within the cells. Therefore, a lower magnification was used to allow us to follow more cells. We found that addition of A-NK resulted in a significant increase of $[Ca^{2+}]_i$ from the resting $[Ca^{2+}]_i$ of 205 ± 102 nM (n=56) to 540 ± 102 nM in 60% (34 of 56) of the observed hepatocytes followed by externalization of the PS. However, in the other 40% no increase in intracellular free calcium occurred before PS were externalized. Moreover, in 17% of the hepatocytes PS were not externalized despite a $[Ca^{2+}]_i$ response.

Discussion

Apoptosis was induced in the hepatocytes after attack by A-NK cells (16) and exposure to ATP (26) or cycloheximide (27). All three conditions resulted in a rapid decrease of the MMP followed by externalization of the PS. As shown in the time-lapse series of the attack by A-NK cells, contact between some hepatocytes and A-NK cells was made after 17 minutes. Already at 32 minutes mitochondria in some areas of the hepatocytes had lost their MMP and at 38 minutes exposure of PS at sites with affected mitochondria began. As is evident from the photo micrographs externalization of PS took place at those areas or sites of the cell where mitochondria had lost their MMP. The most straightforward explanation for PS externalization at these sites is that ATP levels in the immediate surroundings of defective mitochondria rapidly decreases resulting in inhibition of the translocase that normally translocates phosphatidyl serines to the inner leaflet. Unfortunately no cell permeable dyes are yet available to determine local changes in ATP within the cell. ATP has been determined in hepatocytes but this involved microinjection of luciferase and immobilization of the cells in agar that are both conditions that will probably effect membrane structure (34) and interaction of hepatocytes with A-NK cells. Similarly, microinjection of a vector for luciferase (35) will affect membrane structure and in addition it requires cell culture that certainly affects energy metabolism in hepatocytes. Therefore, to discriminate between effects of a collapse of the MMP itself or the resulting decrease in ATP, we chose the approach to deplete ATP from cells while keeping the MMP intact, by treatment of the cells with rotenone. Alternatively we depleted ATP with rotenone in the presence of fructose to replete it again. Under ATP-

depleted conditions the staining for externalized PS co-localized with mitochondrial MMP indicating that PS externalization does not require a collapse in MMP. We found, as reported before (36), that depletion of ATP by itself does not induce apoptosis: an apoptotic signal is needed. Very recently a similar finding was reported: Fas-triggered PS exposure was enhanced by depletion of intracellular ATP (37). In cells incubated with rotenone in the presence of fructose the ATP level remained partly intact but importantly the MMP was at the same level as in control cells indicating that locally generated ATP from fructose is used for maintenance of the MMP. Such a mechanism has been described in osteosarcoma cells with defective mitochondria and is based on reverse action of the ATP synthase (38). The enzyme that ultimately produces ATP from 3-phosphoglycerolphosphate, phosphoglyceratekinase, is located throughout the cytosol and often in the direct vicinity of mitochondria (39). Therefore these organelles have direct access to newly formed ATP. We therefore hypothesize that local produced ATP is used for maintenance of the MMP rather than transported to peripheral regions of the cell.

Only a part of the mitochondrial population in a cell lost its potential in our experiments, resulting in a population of cells that have a relative high overall MMP but do expose PS locally. This is in contrast with the situation in thymocytes and lymphoma cells (6,40) in which the MMP needs to be fully disrupted before externalization of PS occurs. Above we hypothesized that the link between MMP and PS is a local drop in ATP. The ability of cells to generate ATP by mitochondria or glycolysis and the rate of ATP consumption determine the ultimate local ATP level. In particular, local consumption of ATP by mitochondria and the presence of high ATP consumption by the plasma membrane Na^+ -

K^+ and Ca^{2+} -ATPase at the periphery may result in a lower [ATP] in this domain than in the bulk of the cell cytosol (41) This may differ strongly between different cell types and, therefore, influence the coupling between MMP and PS. As the phospholipid translocase is also an ATP-dependent enzyme this may explain why locally, where the mitochondria do not function anymore, PS externalization takes place.

Next to ATP also calcium-dependent processes have been described to play a role in PS externalization: by activation of a calcium-dependent scramblase or synthesis of PS through a calcium-dependent exchange of the polar head group of pre-existing phospholipids. We measured the calcium concentration in hepatocytes loaded with Fura-2 during attack by A-NK cells. ANV and TOTO-3 were added to the medium and, therefore, we could monitor when cells became apoptotic resp necrotic. We found no straightforward relation between elevation of intracellular calcium and PS-exposure. In 60% of the hepatocytes calcium was elevated before exposure of PS but in 40% it was not. Also in a number of cells the calcium levels decreased to base line again before PS exposure occurred. In addition, some hepatocytes had elevated calcium levels but did not exposed PS. Therefore, in the experiments with the A-NK cells the activation of a calcium-activated scramblase is probably not essential (but can not be excluded). Similarly the involvement of calcium-dependent synthesis is doubtful.

In conclusion we show that in hepatocytes during apoptosis mitochondria in certain areas within the cell loose their MMP resulting in local exposure of the PS while in other areas mitochondria remain intact. While the former apparently leads to exposure of PS which is essential for removal of the apoptotic bodies, the latter could be important for proper assembly of cytochrome c, APAF-1, procaspase-9 and ATP into an apoptosome. We

used in this study A-NK cells that secrete the apoptosis-inducing molecules granzyme B/perforin and produce FAS-ligand and TRAIL. In addition, ATP was used which induces an immediate influx of calcium resulting in a loss of MMP (42) and cycloheximide that is a protein synthesis inhibitor. All these stimuli produced the same result and, therefore, the spatial temporal relationship between a decrease in MMP and exposure of PS could be a general phenomenon in cells that depend on mitochondria for their ATP supply.

Legends

Figure 1

Time course of disruption of the MMP and the externalization of PS in isolated hepatocytes exposed to A-NK cells.

Freshly isolated rat hepatocytes were exposed to A-NK cells. Annexin V (ANV) and propidium iodide (PI) were added to hepatocytes that were preloaded with 0.2 mM TetraMethyl Rosamine for 15 minutes; subsequently images of the same cell were taken using video microscopy. At $t=0$ A-NK cells were added and at the indicated time points (in minutes) images were taken of the PS externalization (red ANV staining), MMP (green TMR staining) and morphology. The non-permeable probe PI was added to the cells to verify that the loss of MMP was not caused by a leakage of fluorescent probe due to plasma membrane permeabilization. The upper row shows the merged images of PS externalization and decrease in MMP.

Figure 2

Confocal laser scan photomicrograph of disruption of the MMP and the externalization of PS in isolated hepatocytes exposed to A-NK cells.

Same conditions as in figure 1. TMR was excited with the green laser (A) and ANV with the blue laser (B). These images were pseudo-colored and merged (C). The morphology is shown in (D), arrows indicate apoptotic cells. Hepatocytes were exposed to A-NK cells for 95 minutes.

Figure 3

Confocal laser scan photomicrograph of disruption of the MMP and the externalization of PS in isolated hepatocytes exposed to ATP

Same conditions as in figure 1. Hepatocytes were incubated with 0,4 mM ATP (A) TMR; (B) ANV; (C) merge; (D) morphology is shown in (D), arrows indicate apoptotic cells. Hepatocytes were exposed to ATP for 27 minutes

Figure 4

Confocal laser scan photomicrograph of disruption of the MMP and the externalization of PS in isolated hepatocytes exposed to cycloheximide

Same conditions as in figure 1. Hepatocytes were incubated with 30 µg/ml cycloheximide (A) TMR; (B) ANV; (C) merge; (D) morphology is shown in (D), arrows indicate apoptotic cells. Hepatocytes were exposed to cycloheximide during 55 minutes

Figure 5

ATP concentrations in hepatocytes and MMP exposed to fructose and/or rotenone.

Hepatocytes were incubated and samples were drawn. One half of the sample was immediately frozen in liquid nitrogen. In this sample ATP was determined using the luciferin/luciferase assay. In the other half of the sample the MMP was determined using the flow cytometer. (A) control, (B) 10 µM rotenone, (C) 3 mM fructose, (D) 10 µM rotenone and 3 mM fructose.

Figure 6

Confocal laser scan photomicrograph of disruption of the MMP and the externalization of PS in isolated hepatocytes exposed to A-NK cells after addition of rotenone.

Same conditions as in figure 1. TMR was excited with the green laser (A) and ANV with the blue laser (B). These images were pseudo-colored and merged (C). The morphology is shown in (D), arrows indicate apoptotic cells. Hepatocytes were exposed to A-NK cells for 70 minutes. Twenty minutes after the start of the incubation rotenone was added.

References

1. Kroemer G and Reed JC (2000) Mitochondrial control of cell death. *Nat Med.* 6: 513-509.
2. Paolo Bernardi, Luca Scorrano, Raffaele Colonna, Valeria Petronilli, and Fabio Di Lisa (1999) Mitochondria and cell death: Mechanistic aspects and methodological issues. *Eur J Biochem.* 264: 687-701.
3. Lemasters, J.J., DiGiuseppi, J., Nieminen, A.L. & Herman, B. (1987) Blebbing, free Ca^{2+} and mitochondrial membrane potential preceding cell death in hepatocytes. *Nature* 325, 78–81.
4. Crompton, M., Costi, A. & Hayat, L. (1987) Evidence for the presence of a reversible Ca^{2+} -dependent pore activated by oxidative stress in heart mitochondria. *Biochem. J.* 245, 915–918
5. Crompton, M. & Costi, A. (1988) Kinetic evidence for a heart mitochondrial pore activated by Ca^{2+} , inorganic phosphate and oxidative stress. A potential mechanism for mitochondrial dysfunction during cellular Ca^{2+} overload. *Eur. J. Biochem.* 178, 489–501.
6. Zamzami, N., Marchetti, P., Castedo, M., Decaudin, D., Macho, A., Hirsch, T., Susin, S.A., Petit, P.X., Mignotte, B. & Kroemer, G. (1995) Sequential reduction of mitochondrial transmembrane potential and generation of reactive oxygen species in early programmed cell death. *J. Exp. Med.* 182, 367–377
7. Bernardi, P. (1998) Mitochondria in cell death (preface). *Biochim. Biophys. Acta* 1366, 1–2

8. Zamzami, N., Marchetti, P., Castedo, M., Hirsch, T., Susin, S.A., Masse, B. & Kroemer, G. (1996) Inhibitors of permeability transition interfere with the disruption of the mitochondrial transmembrane potential during apoptosis. *FEBS Lett.* **384**, 53–57.
9. Zamzami, N., Susin, S.A., Marchetti, P., Hirsch, T., Gomez Monterrey, I., Castedo, M. & Kroemer, G. (1996) Mitochondrial control of nuclear apoptosis. *J. Exp. Med.* **183**, 1533–1544.
10. Susin, S.A., Lorenzo, H.K., Zamzami, N., Marzo, I., Snow, B.E., Brothers, G.M., Mangion, J., Jacotot, E., Costantini, P., Loeffler, M., Larochette, N., Goodlett, D.R., Aebersold, R., Siderovski, D.P., Penninger, J.M. & Kroemer, G. (1999) Molecular characterization of mitochondrial apoptosis-inducing factor. *Nature* **397**, 441–446
11. Gores, G.J., Miyoshi, H., Botla, R., Aguilar, H.I. & Bronk, S.F. (1998) Induction of the mitochondrial permeability transition as a mechanism of liver injury during cholestasis: a potential role for mitochondrial proteases.
12. Liu, X., Kim, C.N., Yang, J., Jemmerson, R. & Wang, X. (1996) Induction of apoptotic program in cell-free extracts: requirement for dATP and cytochrome *c*. *Cell* **86**, 147–157
13. Petronelli V, Penzo D, Scorrano L, Bernardi P and Di Lisa F (2001). The mitochondrial permeability transition, release of cytochrome *c* and cell death. Correlation with the duration of pore openings in situ. *J Biol Chem.* **276**:12030-12034
14. Bratton SB and Cohen GM (2001) Apoptotic death sensor: an organelle's alter ego? *Trends Pharmacol Sci.* **22**: 306-315

15. Susin SA, Zamzami N, Castedo M, Daugas E, Wang HG, Geley S, Fassy F, Reed JC and Kroemer G. (1997) The central executioner of apoptosis: multiple connections between protease activation and mitochondria in Fas/APO-1/CD95- and ceramide-induced apoptosis. *J Exp. Med.* **186**: 25-37
16. Blom WM, De Bont HJ, Meijerman I, Kuppen PJ, Mulder GJ, Nagelkerke JF (1999) Interleukin-2-activated natural killer cells can induce both apoptosis and necrosis in rat hepatocytes *Hepatology* **29**: 785-792.
17. Fadok VA, Voelker DR, Campbell PA, Cohen JJ, Bratton DL and Henson PM (1992) Exposure of phosphatidylserine on the surface of apoptotic lymphocytes triggers specific recognition and removal by macrophages. *J Immunol* **148**: 2207-2216.
18. Williamson P and Schlegel RA (1994) Back and forth: the regulation and function of transbilayer phospholipid movement in eukaryotic cells. *Mol.Memb. Biol.* **11**: 199-216.
19. Tang X, Schlegel RA, Halleck M and Williamson P (1996) A subfamily of P-type ATPases with aminophospholipid transporting activity. *Science* **272**: 1495 -1497.
20. Williamson P, Kulick A, Zachowski A, Schlegel RA and Devaux PF (1992) Ca²⁺ induces transbilayer redistribution of all major phospholipids in human erythrocytes. *Biochemistry* **31**: 6355 –6360
21. Williamson P, Bevers EM, Smeets EF, Comfurius P, Schlegel RA and Zwaal RFA (1995) Continuous analysis of the mechanism of activated transbilayer lipid movement in platelets. *Biochemistry* **34**: 10448 –10455

22. Smeets EF, Comfurius P, Bevers EM and Zwaal RFA (1994) Calcium-induced transbilayer scrambling of fluorescent phospholipid analogs in platelets and erythrocytes. *Biochim. Biophys. Acta* **1195**: 281 -286.
23. Pelassy C, Breitmayer JP, Aussel C (2001) Inhibition of phosphatidylserine synthesis in Jurkat T cells by hydrogen peroxide. *Biochim Biophys Acta* **1539**(3): 256-64.
24. Kroemer G, Zamzani N and Susin SA (1997). Mitochondrial control of apoptosis. *Immunol Today*. **18**:44-51.
25. Denecker G, Dooms H, Van Loo G, Vercammen D, Grooten J, Fiers W, Declercq W and Vandenabeele P (2000) P Phosphatidyl serine exposure during apoptosis precedes release of cytochrome c and decrease in mitochondrial transmembrane potential. *FEBS Lett* **465**(1): 47-52.
26. Nagelkerke JF and Zoetewey JP (2001) Purinergic receptor-mediated cytotoxicity. In *Mitochondria in pathogenesis*, Lemasters JJ and Nieminnen AL eds. (New York: Kluwer Academic/Plenum Publishers) pp. 449-464.
27. Blom WM, De Bont HJGM, Meijerman I, Mulder GJ and Nagelkerke JF (1999) The induction of apoptosis in hepatocytes by cycloheximide is prevented by adenosine and caspaseinhibitors. *Biochem. Pharmacol.*, **58**, 1891-1898
28. Nagelkerke JF, Barto KP, Van Berkel TJC (1983) In vivo and in vitro uptake and degradation of acetylated low density lipoprotein by rat liver endothelial, Kupffer, and parenchymal cells. *J Biol Chem* **258**: 12221-12227.
29. Giezeman-Smits KM, Gorter A, Nagelkerke JF, Van Vlierberghe RLP, Van Eendenburg J, Eggermont AMM, Fleuren GJ and Kuppen PJK (1997) Characterisation of three new

- membrane structures on rat NK cells which are involved in activation of the lytic machinery. *Immunobiol.* **197**: 429-443.
30. Rolstad B and Seaman WE (1998) Natural killer cells and recognition of MHC class I molecules: new perspectives and challenges in immunology. *Scand. J Immunol.* **47**: 412-425.
31. Nagelkerke JF and De Bont HJGM (1996) Upgrading of a BioRad MC-600 confocal laser scanning microscope with a 543 nm- and a 633 nm-HeNe laser. *J of Microscopy* **184**: 58-61.
32. Manders EMM, Verbeek FJ and Aten JA (1993) Measurement of co-localization of objects in dual-color confocal images. *J. Microscopy* **169**, 375-382.
33. Smallcombe A and McMillan D. Bio-Rad technical note 11. Co-localization; how it is determined and how it is analyzed.
34. Koop A and Cobbold PH. (1993) Continuous bioluminescent monitoring of cytoplasmic ATP in single isolated rat hepatocytes during metabolic poisoning. *Biochem J.* **295**:165-170
35. Porcelli AM, Pinton P, Ainsrow EK, Chiesa A, Rigolo M, Rutter GA and Rizzuto R (2001) Targeting of reporter molecules to mitochondria to measure calcium, ATP, and pH. *Methods Cell Biol.* **65**:353-380
36. Nicotera P, Leist M and Ferrando-May E (1998) Intracellular ATP, a switch in the decision between apoptosis and necrosis. *Toxicol Lett.* **102-103**:139-142.
37. Gleiss B, Gogvadze V, Orrenius S and Fadeel B (2002). Fas-triggered phosphatidylserine exposure is modulated by intracellular ATP. *FEBS Lett.* **519**:153-158

38. Jiang S, Cai J, Wallace DC and Jones DP. (1999). Cytochrome c-mediated apoptosis in cells lacking mitochondrial DNA. *J Biol Chem* **274**: 29905-29911.
39. Kumble KD and Vishwanatha JK (1991) Immunoelectron microscopic analysis of the intracellular distribution of primer recognition proteins, annexin 2 and phosphoglycerate kinase, in normal and transformed cells. *J Cell Sci.* **99**:751-758.
40. Castedo M, Hirsch T, Susin SA, Zamzami N, Marchetti P, Macho A and Kroemer G. (1996) Sequential acquisition of mitochondrial and plasma membrane alterations during early lymphocyte apoptosis. *J Immunol* **157**:512-521
41. Ashcroft FM and Kakei M (1989). ATP-sensitive K⁺ channels in rat pancreatic beta-cells: modulation by ATP and Mg²⁺ ions. *J Physiol.* 1989 **416**:349-367.
42. Zoetewey JP, van de Water B, de Bont HJGM, Mulder GJ and Nagelkerke JF (1992) The involvement of intracellular Ca²⁺ and K⁺ in dissipation of the mitochondrial membrane potential and cell death induced by extracellular ATP in hepatocytes. *Biochem. J.* **288**, 207-213.


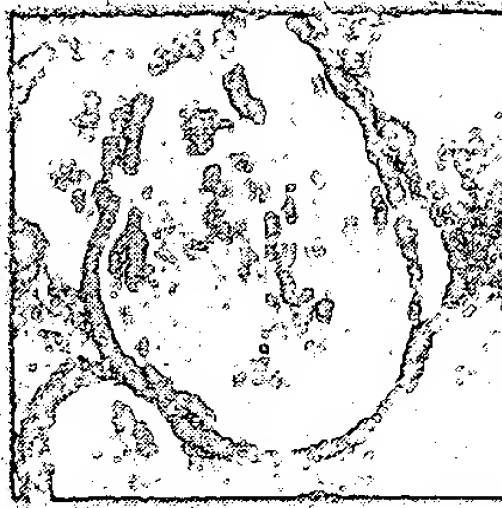




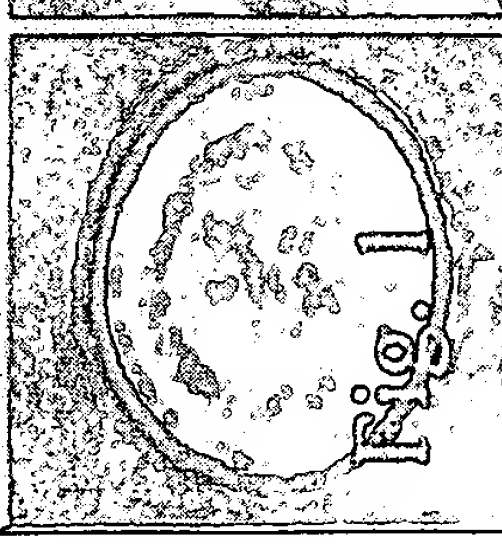
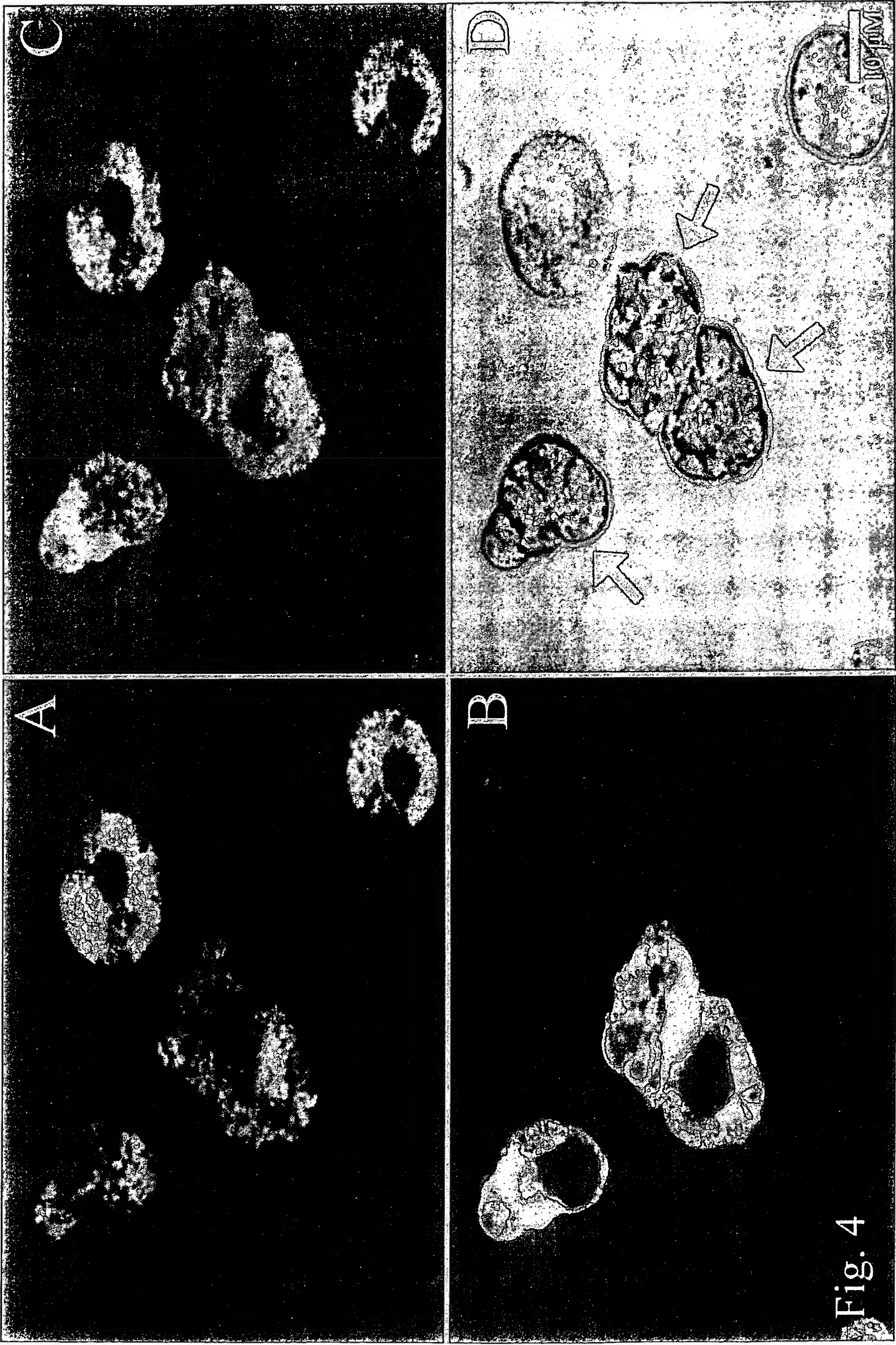
94			
63			
49			
38			
32			
17			
0			

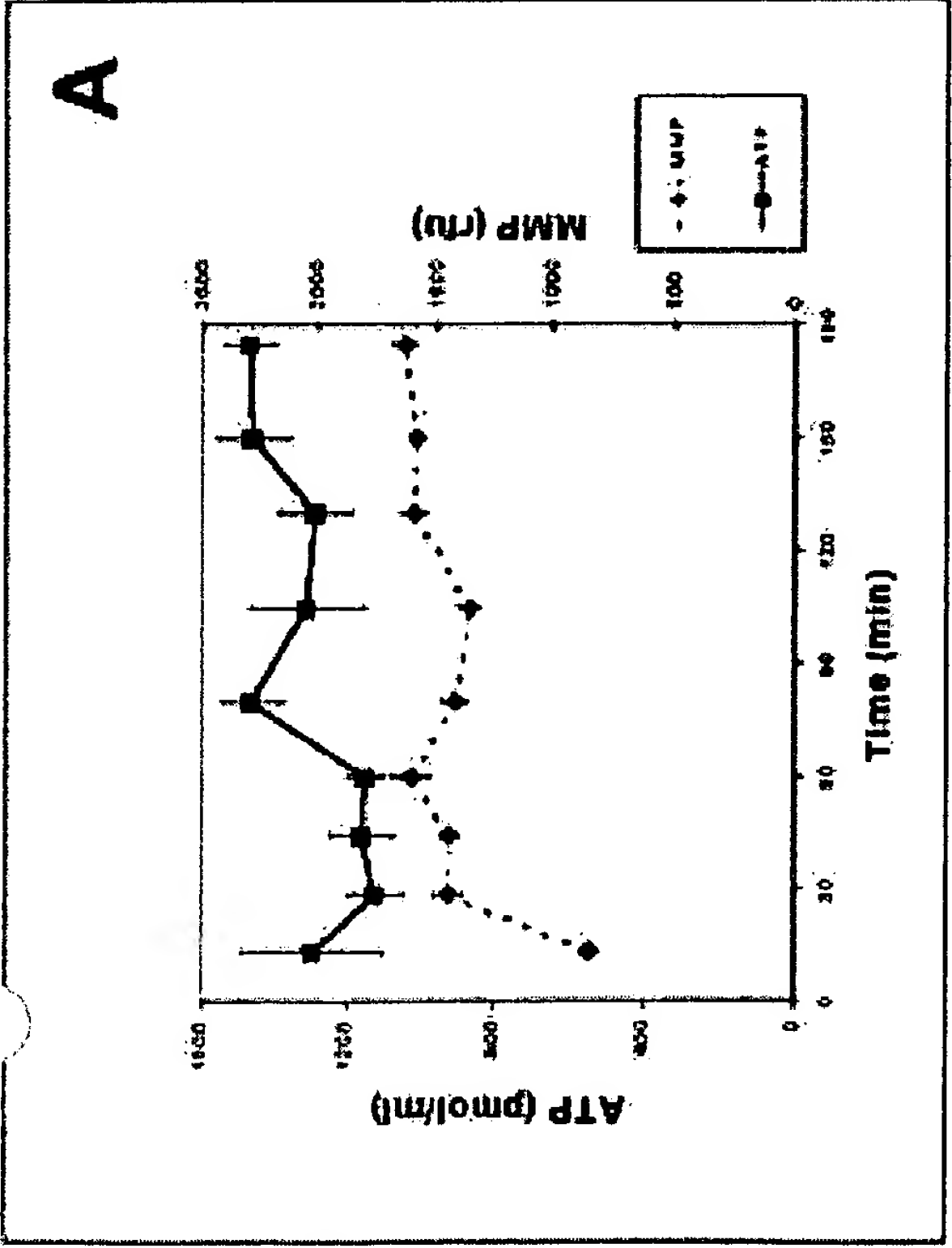
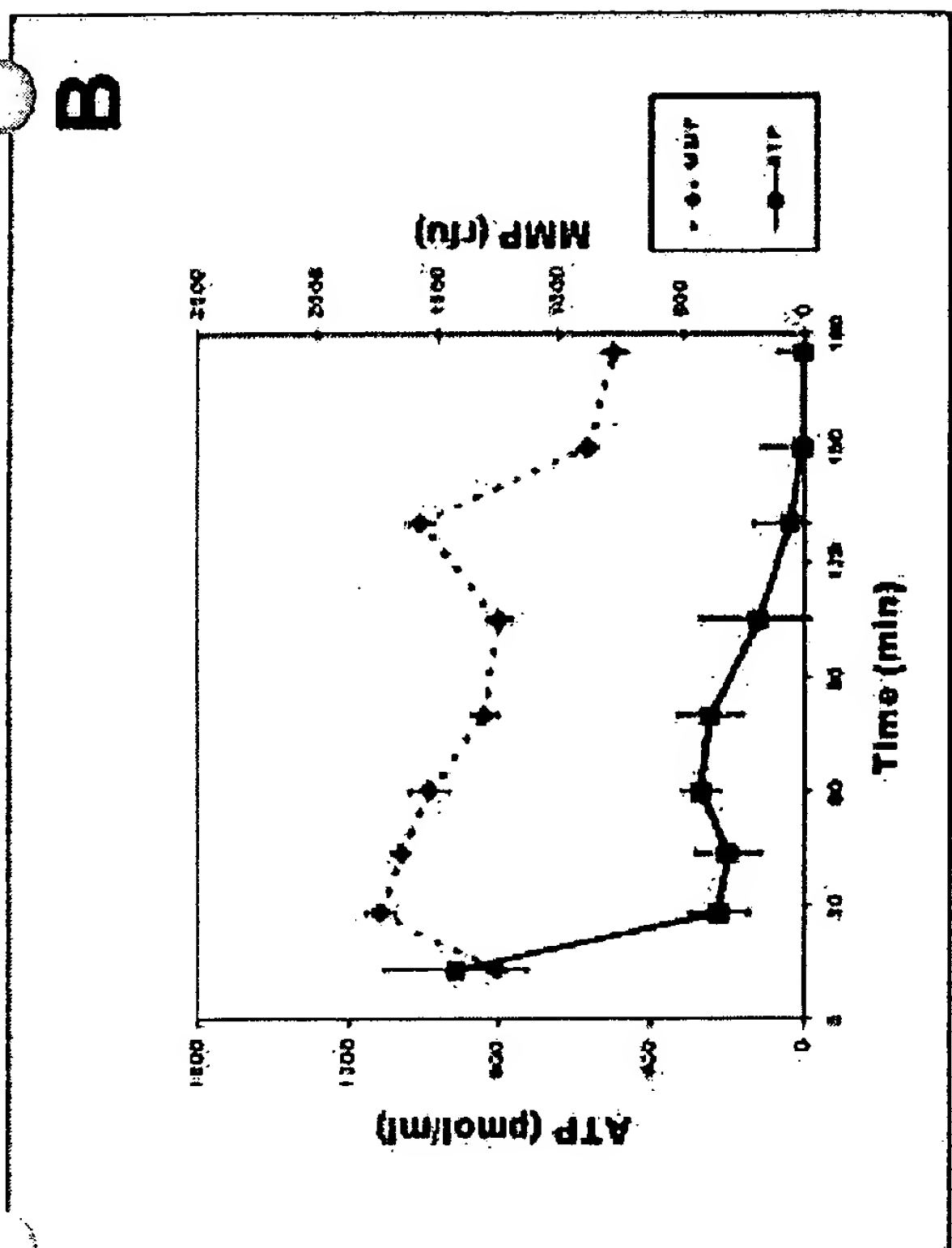
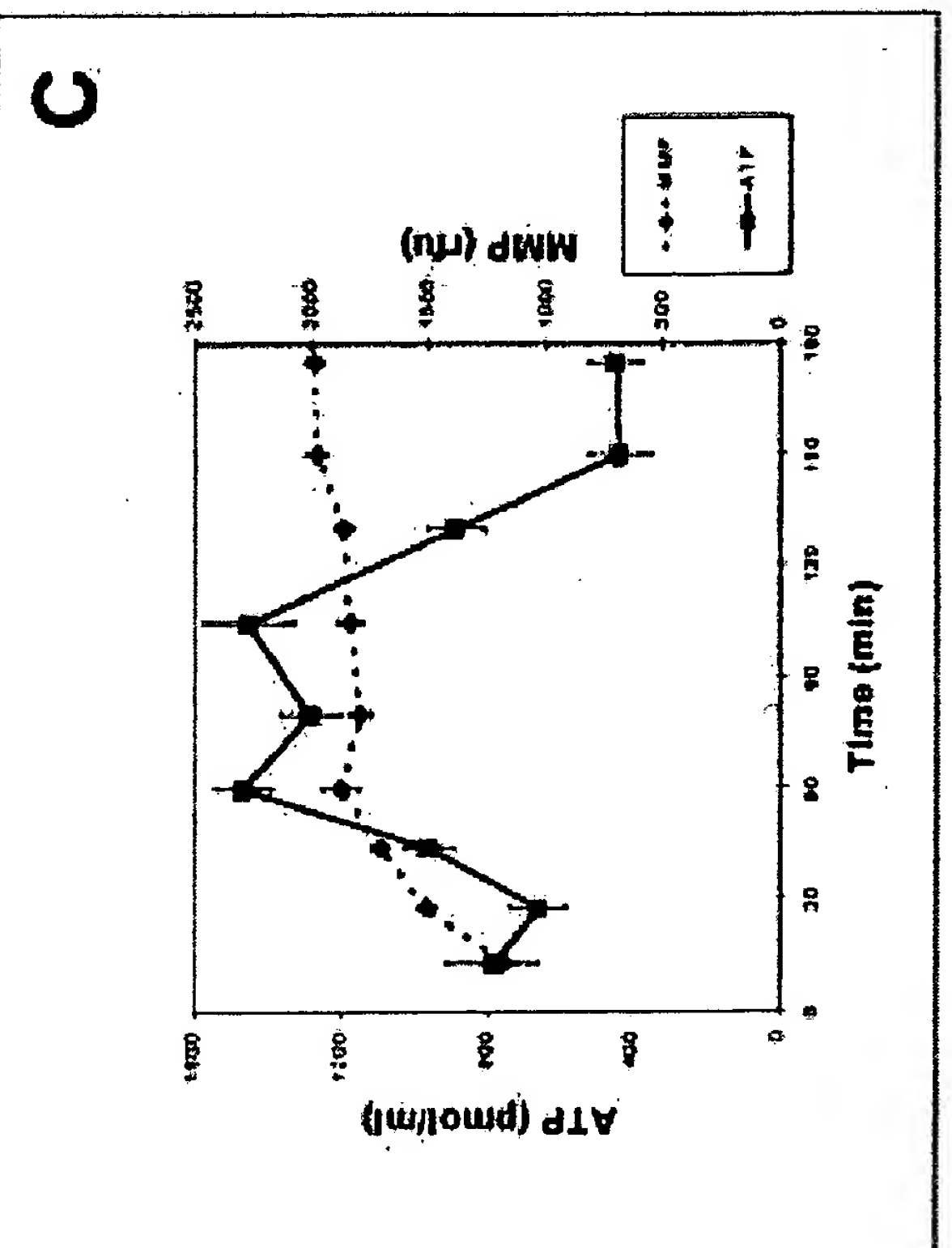
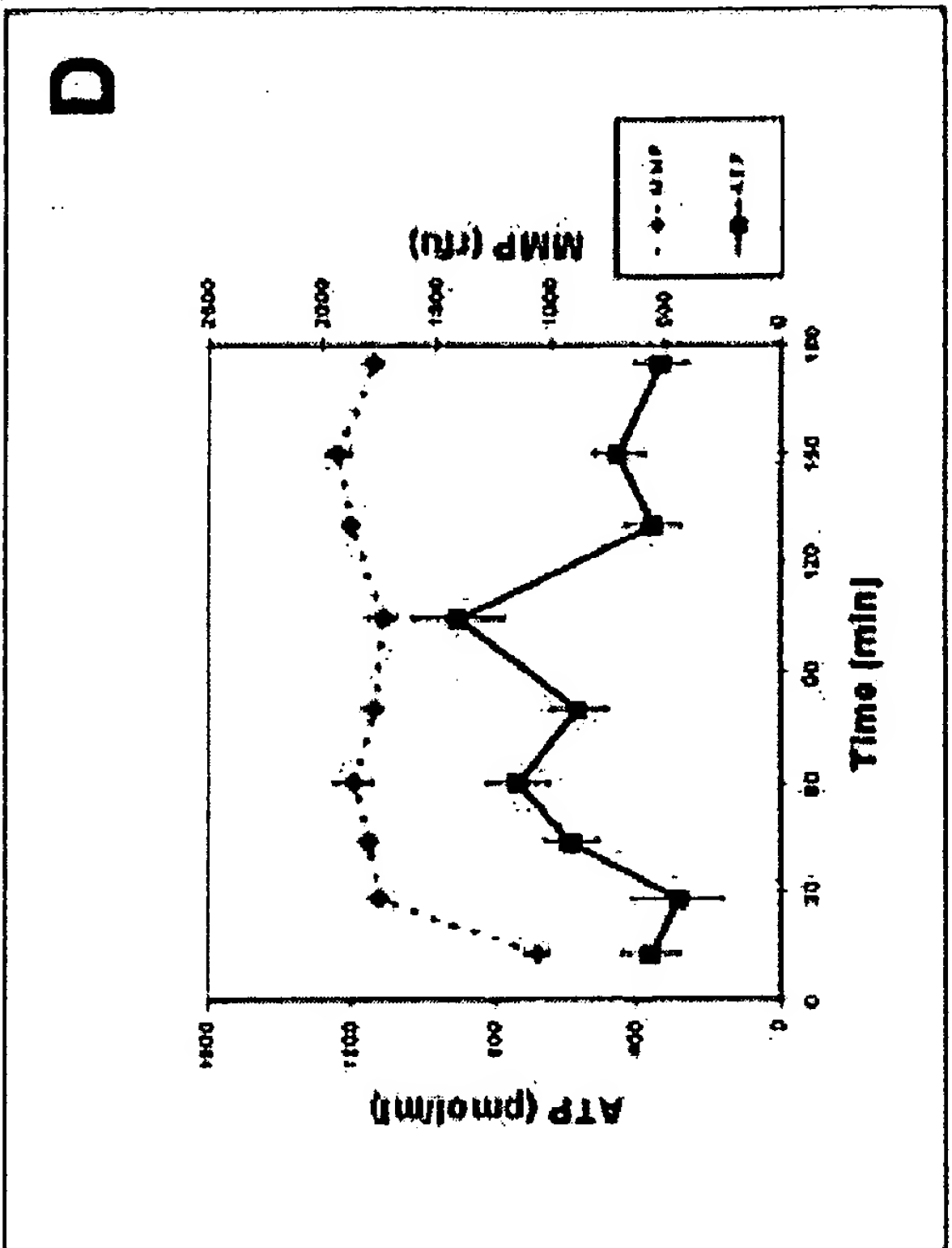


Fig. 2



Fig. 3





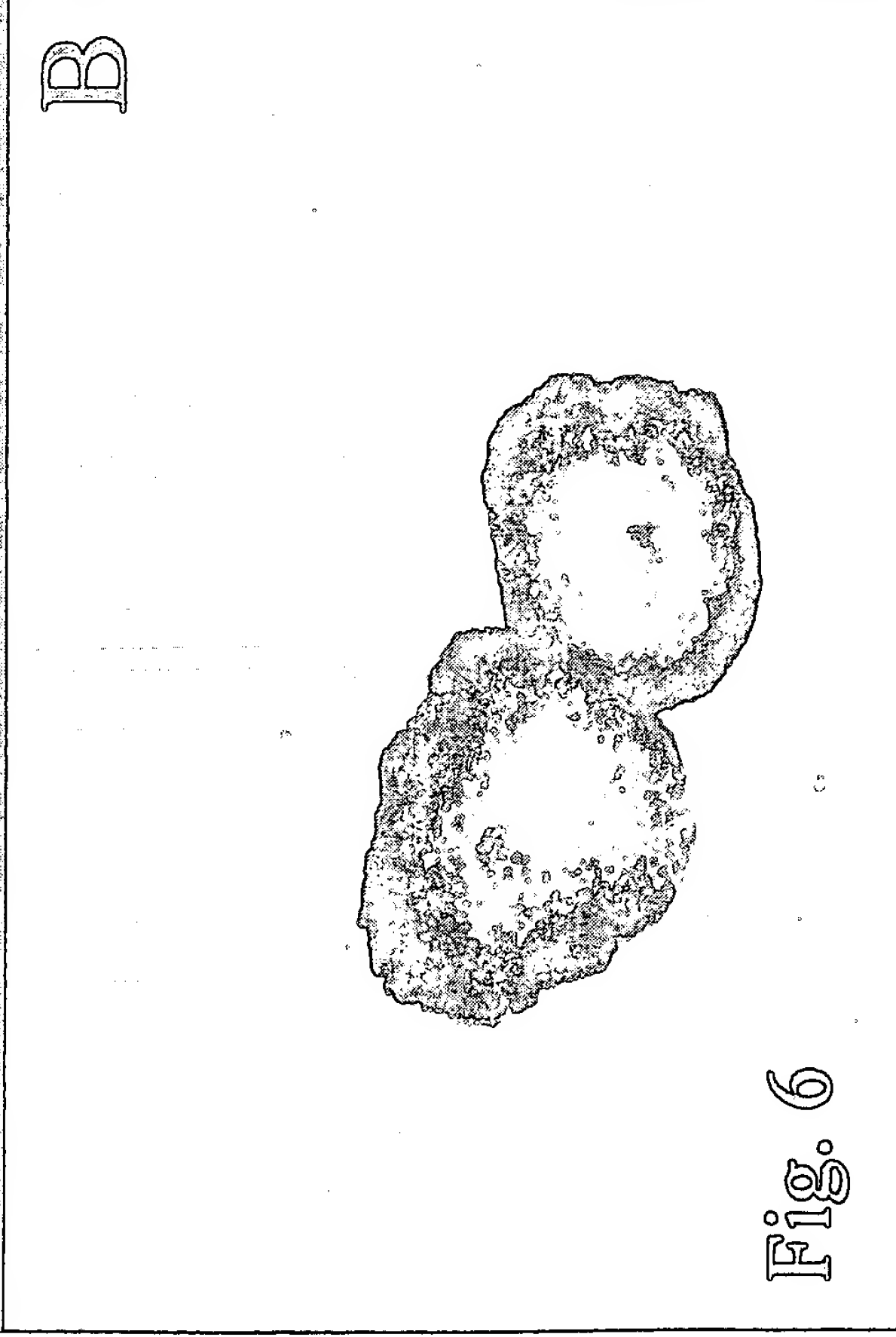
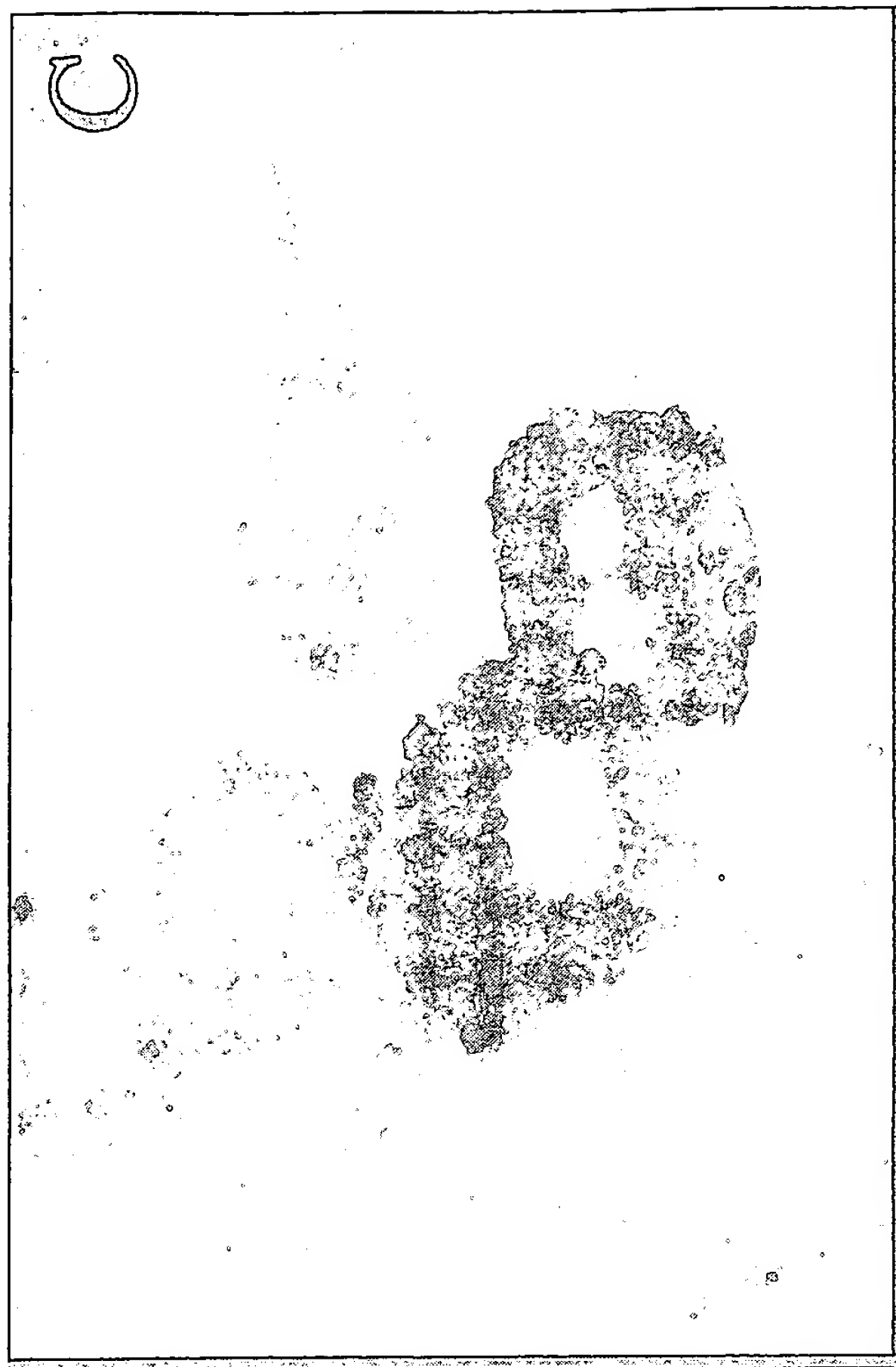
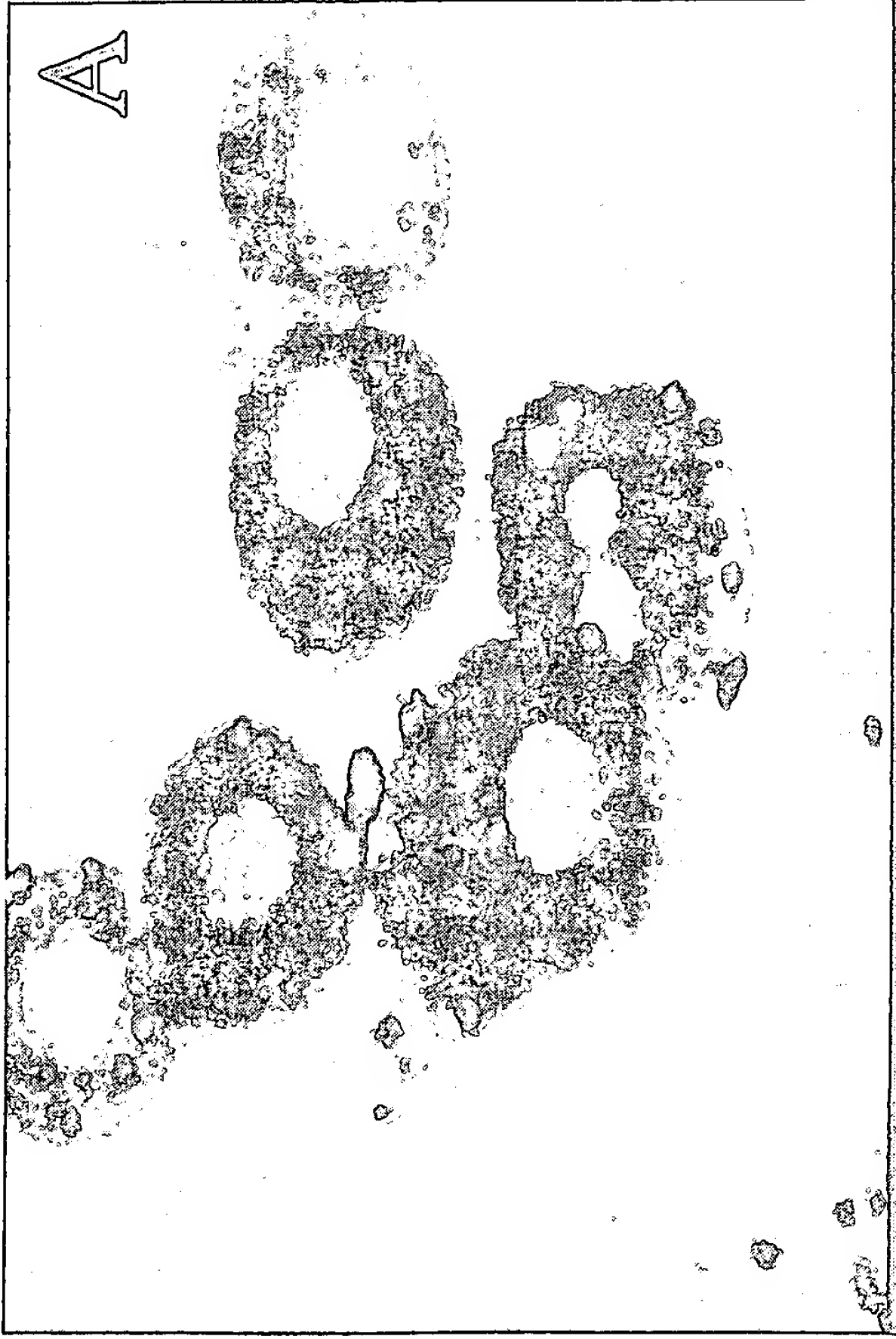


Fig. 6

**This Page is Inserted by IFW Indexing and Scanning
Operations and is not part of the Official Record**

BEST AVAILABLE IMAGES

Defective images within this document are accurate representations of the original documents submitted by the applicant.

Defects in the images include but are not limited to the items checked:

- ☐ **BLACK BORDERS**
- ☐ **IMAGE CUT OFF AT TOP, BOTTOM OR SIDES**
- ☐ **FADED TEXT OR DRAWING**
- ☐ **BLURRED OR ILLEGIBLE TEXT OR DRAWING**
- ☐ **SKEWED/SLANTED IMAGES**
- ☐ **COLOR OR BLACK AND WHITE PHOTOGRAPHS**
- ☐ **GRAY SCALE DOCUMENTS**
- ☐ **LINES OR MARKS ON ORIGINAL DOCUMENT**
- ☐ **REFERENCE(S) OR EXHIBIT(S) SUBMITTED ARE POOR QUALITY**
- ☐ **OTHER:** _____

IMAGES ARE BEST AVAILABLE COPY.

As rescanning these documents will not correct the image problems checked, please do not report these problems to the IFW Image Problem Mailbox.